ELSEVIER

Coordination Chemistry Reviews
208 (2000) 169–191

COORDINATION CHEMISTRY REVIEWS

www.elsevier.com/locate/ccr

DNA-binding studies of Cu(T4), a bulky cationic porphyrin

Patricia Lugo-Ponce, David R. McMillin *

Department of Chemistry, Purdue University, 1393 Brown Building West Lafayette, IN 47907-1393, USA

Received 21 September 1999; received in revised form 17 December 1999; accepted 7 January 2000

Contents

* Corresponding author. Fax: +1-317-4940239.
E-mail address: mcmillin@purdue.edu (D.R. McMillin).

PII: S0010-8545(00)00295-2

Abstract

The potential for therapeutic applications has provided much of the impetus for investigating the DNA-binding interactions of cationic metalloporphyrins, but there are also signs of intriguing base and sequence dependences. More recent work has established that the stem regions of DNA hairpins are extremely useful as model duplexes. Mainly the focus has been on 16-mers with generic sequence 5′-GANNAC-NNNN-GTNNTC-3′, where the letters A, C, G, and T denote adenine, cytosine, guanine, and thymine nucleotides, respectively. N is the symbol for a variable nucleotide in the string; and the inner dashes enclose the loop sequence: TTTT, GTTA or GAAA. Because of its spectroscopic properties, the porphyrin of interest has been Cu(T4), the Cu(II) derivative of H_2T4 (H_2T4, *meso*-tetrakis(4-(*N*-methylpyridiniumyl))porphyrin). Spectral data have revealed that the hairpins retain their stem structures in the adducts with Cu(T4) and have provided important new insights into the interactions that occur. One is that the local rigidity of the DNA is the most important factor that shapes the binding. A run of DNA that includes at least 50% G≡C base pairs can support intercalative binding with or without contiguous G≡C base pairs in the sequence. As demonstrated by inosine-for-guanine base replacement experiments, the real pre-requisite for intercalative binding is a robust hydrogen bonding framework that overcomes the steric strain generated within the minor groove by pyridyl substituents pressing against the sugar–phosphate backbones. Cu(T4) binds externally to DNA that is richer in the more flexible A=T base pairs. The intercalated form of Cu(T4) is unique in exhibiting an appreciable photoluminescence signal, and the intensity appears to increase with the rigidity of the overall DNA structure. Changes in the stability of the loop structure can perturb external binding interactions as indicated by the shape of the porphyrin's induced circular dichroism (CD) signal. However, the stem composition determines whether intercalation or external binding occurs, though these two adducts may actually be the limiting structures of a continuum of binding motifs. One technique rarely suffices to characterize an adduct but the combination of absorbance, emission and CD spectroscopies is very powerful.

1. Background

1.1. Porphyrins and DNA

Cationic, water-soluble porphyrins, like H_2T4 and various metal-containing derivatives, have received a great deal of attention because they are versatile DNA-binding agents [1–4] (for structures, see Scheme 1). (H_2T4, *meso*-tetrakis(4-(*N*-methylpyridiniumyl))porphyrin). In addition to binding to normal B-form DNA, recent studies have shown that H_2T4 binds to higher-order multi-stranded structures [5], an effect that could prove useful in inhibiting tumor growth [6]. Other work has demonstrated that such porphyrins can exhibit antiviral activity [7] or act as artificial nucleases [8]. With a visible absorption spectrum that extends well into the red spectral region, the porphyrin chromophore also holds great promise as a sensitizer in the area of photodynamic therapy [9–12]. Intracellular targeting may be possible with cationic porphyrins, such as H_2T4 and Cu(T4), because their net

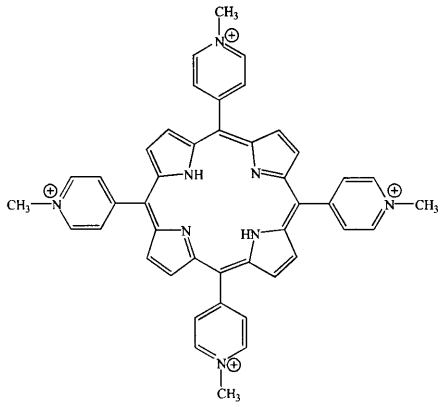

H_2T4

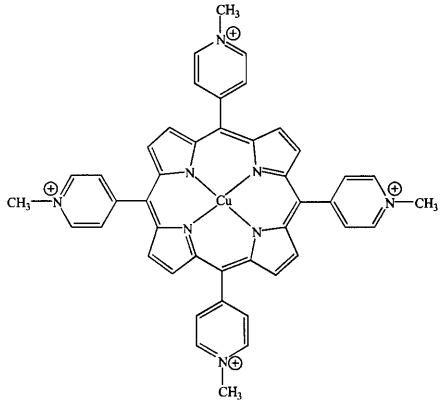

Cu(T4)

Scheme 1.

positive charge should foster migration to the DNA within the nucleus. As the photoinduced cytotoxicity arises from the sensitization of singlet oxygen, Cu(T4) itself is not a very effective agent due to a relatively short excited-state lifetime [13]. However Cu(T4) is a useful spectroscopic probe that can provide information about biodistributions, binding modes and binding affinities of such systems.

Circular dichroism (CD) studies have been instrumental in establishing that multiple types of binding to DNA are possible. Twenty years ago, Fiel and co-workers made the surprising conclusion that H_2T4 could intercalate into DNA with some selectivity for guanine–cytosine (G≡C) base pairs [14,15]. Marzilli and co-workers later showed that Ni(T4) was capable of intercalative binding as well, but that Zn(T4) adopted some type of external binding mode instead [16]. As a rule, intercalative binding induces a negative CD signal in the Soret region, while external, or groove, binding generally induces a positive signal [17]. Pasternack and co-workers used these results to argue that, for obvious steric reasons, metalloporphyrins with one or more axial ligands always bind externally [18]. Carvlin and Fiel detected a third CD signature when they studied modest loadings of H_2TAP, the porphyrin derivative with 4-(*N*,*N*,*N*-trimethylaniliniumyl) substituents in plane of the 4-(*N*-methylpyridiniumyl) groups of H_2T4 [19]. In this instance the induced CD is bisignate in the Soret region with the crossover falling at the wavelength of the absorption maximum. Porphyrin–porphyrin interactions involving chirally related chromophores give rise to such so-called conservative signals, and Fiel and co-workers attributed the effect to self-stacked porphyrins oriented roughly perpendicular to the helix axis [19].

Other techniques also provide insight into the nature of the binding interactions. In the adsorption spectrum, intercalative binding produces a 10–15 nm bathochromic shift of the Soret maximum and a hypochromic effect that can exceed 30% [1,4]. In contrast, external binding produces a small hypochromism, or even hyperchromism, and a comparatively small bathochromic shift of 4 or 5 nm.

Linear dichroism can provide information about the orientation of the bound porphyrin [20]. Marzilli et al. also found that intercalative binding induces a characteristic downfield shift of a phosphate peak in the ^{31}P-NMR spectrum [21]. Using fluorescence methods, Kelly and co-workers have shown that the signal from H_2T4 sharpens on binding to DNA and that external binding produces a marked increase in the emission intensity [23]. The same authors also suggested that electron transfer from guanine might explain the quenching evident in the signal from the intercalated form. McMillin and co-workers investigated the luminescence of the Cu(T4) chromophore itself [24]. In aqueous solution Cu(T4) gives a virtually undetectable emission signal due to an associative, solvent-induced quenching interaction. However, in the presence of DNA, the complex is emissive and the signal intensity increases in proportion to the percentage of G≡C base in the sample. Furthermore, with a random-sequence sample, like the DNA from salmon testes, the absorption spectrum shows that both groove binding and intercalative binding occur, but the excitation spectrum tracks the absorption spectrum of intercalated Cu(T4) [24]. Intercalation into B-form DNA blocks approaches to the axial coordination sites and prevents chemical interactions that would otherwise quench the emission.

1.2. Sequence specificity

Early on, there were indications that H_2T4 intercalates preferentially in regions rich in G≡C base pairs [14,16,18,25]. Footprinting studies later confirmed that groove-binding M(T4) species protect A=T rich regions of DNA, whereas intercalators, like Ni(T4) and Cu(T4), also protect G≡C rich domains [26,27]. On the basis of elegant NMR studies, Marzilli and co-workers then presented evidence that, of the ten different steps that occur in DNA, only the 5′-CpG-3′ sequence supported intercalation of H_2T4 [21], though Ni(T4) was less selective [28]. Subsequent work has shown that the intercalation of H_2T4 does not necessarily require a CpG step [29,30]. In the case of Cu(T4), luminescence results indicate that intercalative binding is feasible as long as the sequence is rich in G≡C base pairs even if they do not occur in succession [24]. On the other hand, time-resolved Raman studies by Nakamoto and co-workers established that external binding of Cu(T4) occurred even in the presence of long runs of G≡C base pairs as long as there was an internal run of at least four consecutive adenine–thymine (A=T) base pairs [22]. For intercalative binding, steric considerations could be the basis of any sequence specificity [31]. The conflicting results described above and the paucity of data pertaining to specific sequences of B-form DNA provided the motivation for the investigations described below.

1.3. Hairpin substrates

In nature, hairpins are common structural elements involved in RNA function [32], gene regulation [33,34], and possibly translation errors associated with heritable diseases [35]. In practice, any oligonucleotide that contains two properly spaced

and oriented, complementary runs of bases is capable of forming a hairpin, although formation of a budged dimer can be a competitive process [33,36,37]. However, the same sequences occur in the double helical regions of the hairpin and the bulged dimer.

The DNA sequence has an important impact on the stability of the hairpin structure. The loop typically involves four or five bases [38], and a run of four thymine residues — a [T4] loop — is relatively stable [39]. However, a [GNRA] loop sequence is even more favorable where N designates any nucleotide, and R designates a purine residue (G or A) [38,40]. The presence of a C≡G base pair next to the loop adds further stability, especially if the cytosine is on the 5′ side of the loop [38,40,41]. A number of NMR-based structures show that a 16-mer with a central run of four thymines forms a stable hairpin with as few as two G≡C base pairs in the stem [41,42].

From the outset [43], hairpin-forming 16-mers have been the vehicle of choice for studies with Cu(T4) and H_2T4. One reason is that the six-base-pair stem is long enough to support groove binding. The focus is on the stem because studies described below show that the loop sequence plays a secondary role in shaping the binding interactions. Although optical studies involving techniques like CD and emission spectroscopy do not provide detailed structural information, they have proved very useful for obtaining information about the mode of interaction and the degree of internalization that occurs.

2. Experimental

2.1. Materials

The oligonucleotides came from the Purdue University Oligonucleotide Macromolecular Structure Facility or IDT Co. (Coralville, IA). The chloride salt of CuT4 was available from a previous study [43]. Worthington Biochemistry Corp. (Lakewood, NJ) supplied the DNase I enzyme, while the dichlorodimethylsilane was from Aldrich Chemical Co. (Milwaukee, WI). The reagent buffer salts came from standard chemical supply houses. For the purification of oligonucleotides, the Poly-Pak cartridges came from Glen Research Corp. (Sterling, VA). The typical substrate is a 16-mer with self-complementary ends:

$$\mathrm{TT} = \begin{matrix} 5'\text{-GA}\mathbf{TT}\text{AC}^{\mathrm{T}}\text{T} \\ 3'\text{-CT}\mathbf{AA}\text{TG}_{\mathrm{T}}\text{T} \end{matrix}$$

Most of the work to date has focused on substitutions at the position marked in bold in the schematic structure, i.e. residues 3, 4, 13 and 14. The letters that code for nucleotides 3 and 4 (TT in the illustration) serve as a shorthand label for a

particular hairpin. The more comprehensive designation TT[T4] includes the composition of the loop in square brackets where in this instance the loop sequence is 5′-TTTT-3′. Two other sequences served as single stranded controls, PU, 5′-GAGAAGTTTT-3′; and PY, 5′-CTCTTCTTTT-3′. Table 1 contains a list of the sequences employed along with a summary of properties.

Table 1
Definitions and properties of hairpin substrates

Hairpin	Stem	Loop	ε[a]/mM^{-1} cm^{-1}	T_m/°C (T')[b]
PU	5′-GAGAAC	TT	89	
		TT		
PY	5′-CTCTTC	TT	65	
		TT		
GC[T4][c]	5′-CAGCAC	TT	132	75
	3′-GTCGTG	TT		
CG[T4]	5′-CACGAC	TT	135	74 ($\geq$82)
	3′-GTGCTG	TT		
CG[GA3]	5′-CACGAC	GA	145	
	3′-GTGCTG	AA		
CG[GT2A]	5′-CACGAC	GT	147	
	3′-GTGCTG	AT		
TT[T4]	5′-CATTAC	TT	142	51 (63)
	3′-GTAATG	TT		
TT[GA3]	5′-CATTAC	GA	166	61
	3′-GTAATG	AA		
TT[GT2A]	5′-CATTAC	GT	151	67
	3′-GTAATG	AT		
AT[T4]	5′-CAATAC	TT	147	55 (62)
	3′-GTTATG	TT		
AT[GA3]	5′-CAATAC	GA	153	66
	3′-GTTATG	AA		
AT[GT2A]	5′-CAATAC	GT	149	66
	3′-GTTATG	AT		
AT[T4][c]	5′-AGATAC	TT	145	56
	3′-TCTATG	TT		
CA[T4][c]	5′-CACAAC	TT	109	65
	3′-GTGTTG	TT		
AG[T4][c]	5′-CAAGAC	TT	149	61
	3′-GTTCTG	TT		
AI[T4][d]	5′-CAAIAC	TT	117	53
	3′-GTTCTG	TT		
CI[T4][d]	5′-CACIAC	TT	124	50
	3′-GTGCTG	TT		
IC[T4][d]	5′-CAICAC	TT	135	50
	3′-GTCITG	TT		

[a] At 260 nm.
[b] T' is the melting temperature with Cu(T4) at Hp/Cu = 1.
[c] Ref. [43].
[d] Refs. [54,70].

2.2. Methods

Treatment of glassware with dichlorodimethylsilane helped to minimize the adsorption of porphyrin [44]. In conjunction with the data for individual nucleotides, digestion with DNase I in pH 7.9 Tris buffer allowed the estimation of molar extinction coefficients for the various hairpins [45]. The buffer for most of the spectral studies was a $\mu = 0.1$ phosphate buffer (pH 6.8) containing 0.05 M NaCl. The chromatographic purification of an oligonucleotide, which initially retained a terminal trityl substituent, followed standard procedures. After a precipitation step with ethanol, it is possible to dissolve the hairpin in any buffer of interest. For the titrations, the Cu(T4) concentration was typically 1.7 μM throughout the experiment. The excitation wavelength for the emission experiments was 434 nm. The filter arrangement had a 452 nm notch filter in the excitation beam and a 510 nm long-pass filter in front of the detector slits. The bandpass settings for the excitation and emission monochromators were 20 nm. The procedure used to correct for variations in the absorption intensity involved dividing the emission intensity by $(1 - 10^{-A(434)})$, where A(434) denotes the absorbance of the sample at the excitation wavelength. The spectral band width was 1.0 nm for the CD measurements, and data collection with the 50 mdeg range setting gave the best baseline. The method for changing the readings to a molar absorptivity scale involved the formula, $S' = S$ (mdeg)/(32.98 × L × C), where S (mdeg) is the original signal, L is the pathlength of the cell, and C is the concentration of sample.

For the thermal melting studies, all run in aerated solutions, the room-temperature absorbance was around 0.3. A thermistor probe in an adjacent cell block provided the temperature reading. The temperature at which the extremum in the derivative of the absorbance–temperature curve occurred served as the estimate for the melting temperature (T_m). When Cu(T4) was present, the monitoring wavelength was 424 nm, whereas 260 nm was the operative wavelength for the free hairpins. The samples containing free hairpin included a blanketing layer of mineral oil to minimize the rate of solvent evaporation. The scan rate was always 1.0°C min^{-1}.

2.3. Instrumentation

A Perkin Elmer Lambda 4C spectrophotometer or a Cary 100 Bio UV–Visible spectrophotometer with a variable temperature accessory provided the absorbance measurements. The emission spectrofluorometer was an SLM-Aminco SPF-500C, and the CD instrument was a Jasco J-600 Spectropolarimeter. The centrifuge was a Beckman Microfuge II, and the pH meter was a PHM 64 unit.

3. Results

3.1. Absorbance and emission data

Spectral titrations confirmed that formation of the one-to-one adduct of Cu(T4) with the PU or PY oligonucleotide was complete at an oligonucleotide-to-copper ratio of five (Hp/Cu = 5). With either PU or PY the spectra in Fig. 1 reveal that upon uptake the Soret band undergoes a small bathochromic shift and decreases in intensity. However, the hypochromic response is clearly larger for PU, which includes purine bases. Fig. 2 shows that the interaction with PU also induces an emission signal, but the intensity is quite weak.

Pronounced spectral changes also occurred with the addition of a hairpin to solutions containing Cu(T4). Within the CG series, the spectral data for the CG[GA3] system are representative and reveal that at least two different types of adducts form depending on the amount of hairpin in solution (Fig. 3). Thus, the absorbance goes through a minimum and then approaches a limiting value as the hairpin-to-porphyrin ratio increases. At the same time the bathochromic shift of the Soret band evolves in a more monotonic fashion. Qualitatively, the same trends occur with the other CG hairpins and with the PU and PY oligonucleotides as well. For the series of CG hairpins, there is also a noticeable variation in hypochromism (H) of the adducts as well as differences in the emission intensities (Table 2). In contrast to the above, the Soret band exhibits hyperchromism in the presence of an excess of a TT hairpin (Fig. 4). Except with the TT[GT2A] system, the absorbance changes grow in smoothly as the concentration of DNA increases. With TT[GT2A], the hyperchromic response becomes evident a little before the bathochromic shift begins to develop. All the adducts with the TT hairpins exhibit extremely weak

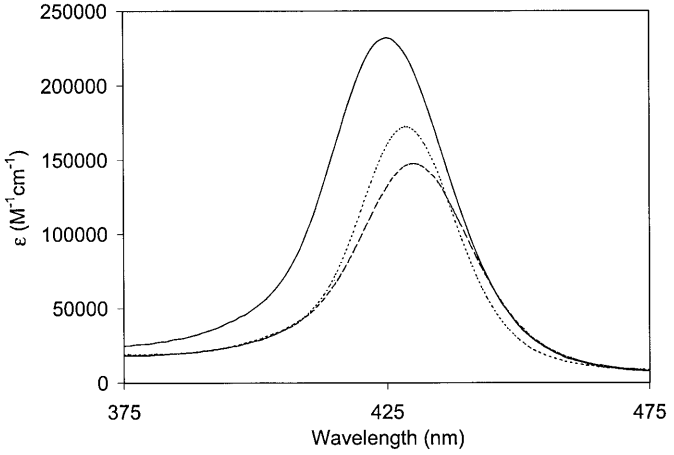

Fig. 1. Soret band of Cu(T4) in the presence of single-stranded DNA. Free porphyrin (—), complex PY at Hp/Cu = 5 (- - -), complex with PU at Hp/Cu = 5 (– –). All spectral studies employed, $\mu = 0.1$ M pH 6.8 potassium phosphate buffer containing 0.05 M NaCl.

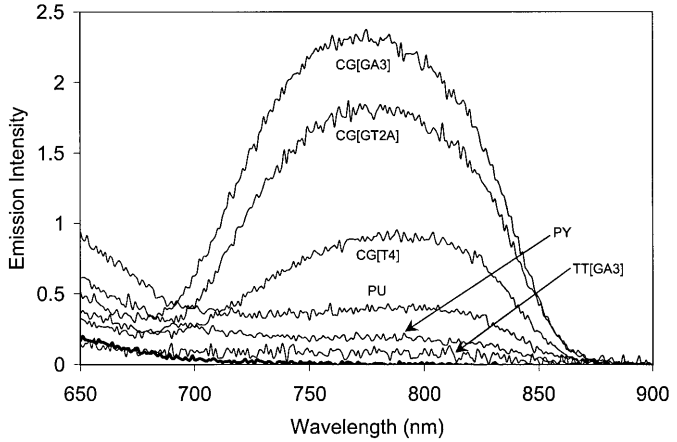

Fig. 2. Emission spectra of Cu(T4). In order of decreasing intensity, the spectra come from solutions containing CG[GA3], CG[GT2A], CG[T4], PU, PY,TT[GA3], and Cu(T4) by itself (thick line). Except for the control, all at Hp/Cu = 5.

emission intensities from the bound porphyrin. The final absorbance changes with the AT hairpins also exhibit hyperchromism (Table 2). Although the spectral response varies with the ionic strength, there is no consistent trend. With, for example, the AT system AT[GT2A] induces a larger hyperchromic response at $\mu = 0.01$ than at $\mu = 0.1$, but the opposite is true with the AT[T4] hairpin. The emission intensities are quite weak for all adducts with AT hairpins (Fig. 2 and Table 2).

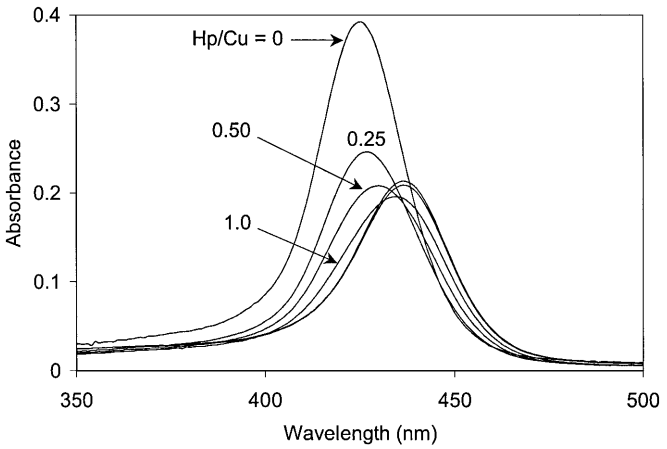

Fig. 3. Absorption spectra of Cu(T4) in the presence of CG[GA3] hairpin. The Soret maximum shifts to longer wavelength as Hp/Cu increases through the series, 0 (no DNA) 0.25, 0.5, 1.0, 5.0, and 9.0. The Hp/Cu = 5 and Hp/Cu = 9 samples have the same λ_{max}.

3.2. CD spectroscopy

Although Cu(T4) is not chiral, interaction with DNA can induce a CD signal. In the case of PY the bound form of Cu(T4) gives no significant response in the Soret region, but the addition of excess PU does induce a weak negative CD signal at around 435 nm (Table 2). As Table 2 also shows, the addition of a CG hairpin induces a much stronger signal. The signal generally grows in at a fixed wavelength, except with CG[T4] where the CD band occurs at longer wavelengths for low values of Hp/Cu (Fig. 5). With the TT hairpins the CD signals are very different. In the presence of excess porphyrin, the TT[T4] hairpin induces a bisignate CD with a total amplitude of about 40 M^{-1} cm^{-1} and a crossover wavelength that coincides with the absorption maximum (Fig. 6). By Hp/Cu = 5, however, the CD signal evolves into a positive band shifted to a shorter wavelength (421 nm). The other two TT hairpins give qualitatively similar results (Table 2) except that the bisignate

Table 2
Physical data for adducts of Cu(T4) in $\mu = 0.1$ pH 6 8 phosphate at Hp/Cu = 5

Hairpin	Absorption		CD		Emission[a]
	$\Delta\lambda$[b]/nm	H[c]/%	λ/nm	$\Delta\varepsilon/M^{-1}$ cm^{-1}	I_{rel}
PU	5	36	432	−5	0.2
PY	4	25			0.1
GC[T4][d]	8	20	433	−22	1.0
CG[T4]	10	26	434	−24	0.9
CG[GA3]	14	45	434	−25	2.0
CG[GT2A]	12	36	433	−22	1.7
TT[T4]	4	−24	421	12	0.1
TT[GA3]	3	−18	420	6	<0.1
TT[GT2A]	3	−12	419	8	<0.1
AT[T4]	4	−18	418	11	0.2
AT[GA3]	3	−6	413	4	0.1
			433	−8	
AT[GT2A]	4	−4	414	3	0.1
			425	−3	
AT[T4][d]	5	10	413	5	0.2
			440?		
CA[T4][d]	7	12	434	−17	0.5
AG[T4][d]	9	25	434	−17	0.7
AI[T4][e]	5	−5	428	−10	0.1
CI[T4][e]	4	−9	424	16	<0.1
IC[T4][e]	6	9	432	−13	0.2

[a] The relative emission intensity I_{rel} comes from a comparison of the emission heights at λ_{max} in the uncorrected emission spectra [43].
[b] Shift of λ_{max} from 424 nm, the wavelength of the Soret maximum for free Cu(T4).
[c] The hypochromism is the percent change of molar absorptivity at the Soret maximum.
[d] Ref. [43].
[e] Ref. [54].

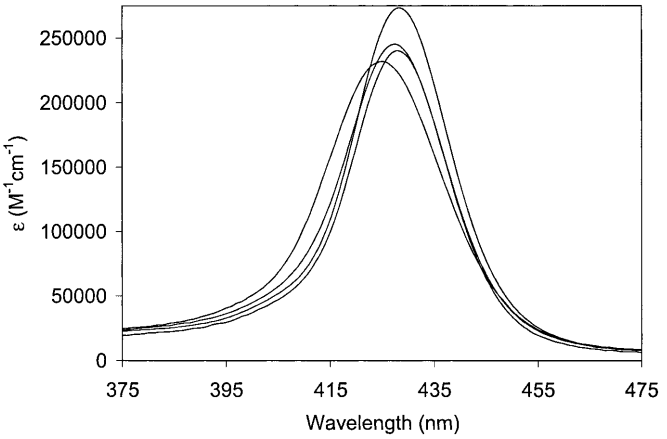

Fig. 4. Soret band of Cu(T4) in the presence of TT hairpins. In order of decreasing intensity the samples contain, TT[T4], TT[GA3], TT[GT2A] and no DNA. Except for the control, Hp/Cu = 5.

character is less evident during the early stages of the titration. The results with the AT[T4] system essentially parallel those of TT[T4], but the other two AT hairpins behave differently. As Fig. 7 reveals, the adducts with AT[GT2A] and AT[GA3] give CD signals that are bisignate even in the presence of a large excess of hairpin.

In the UV region the CD spectra also depend on the hairpin-to-porphyrin ratio. However, the molar absorptivities of the hairpin and porphyrin are similar in this region, so that there is no clear distinction between the signals from the host and the guest. There is, nonetheless, one trend that seems evident and that would be worth further scrutiny. The effect is most evident in the vicinity of 280 nm where

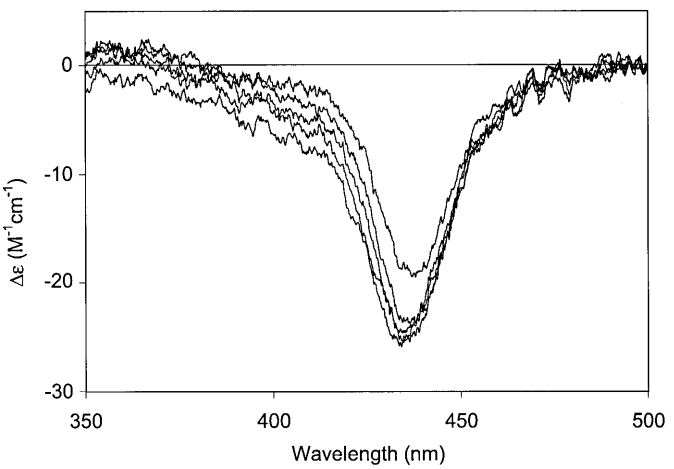

Fig. 5. Induced CD signals from Cu(T4) in the presence of varying amounts of CG[T4]. The negative CD signal becomes more intense as Hp/Cu increases through the series, 0.25, 0.50, 1.0, 5.0 and 9.0,

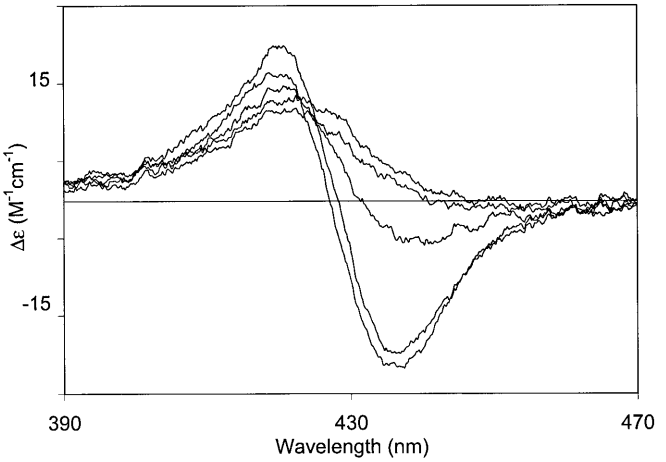

Fig. 6. Induced CD signals from Cu(T4) in the presence of varying amounts of TT[T4]. The total amplitude of the signal decreases as Hp/Cu runs through the series, 0.25, 0.50, 1.0, and 9.0.

all the hairpins exhibit a positive CD signal (An associated trough appears at ca. 250 nm in the CD spectrum, and a crossover occurs at around 260 nm, the position of an absorbance maximum). The CG hairpins are unique in that the addition of Cu(T4) produces an increase in $\Delta\varepsilon$ at 280 nm. In contrast, there is generally a diminution of the $\Delta\varepsilon$ value with the other hairpins in the absence of significant porphyrin–porphyrin interactions, vide infra. See Fig. 8 for representative spectra.

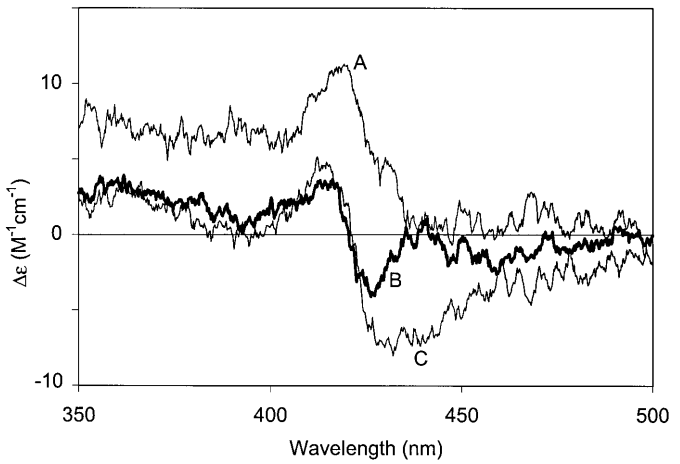

Fig. 7. Induced CD signals from Cu(T4) in the presence of AT hairpins at Hp/Cu = 5. A, With AT[T4] (—); B, with AT[GT2A] (—); and C, with AT[GA3] (—).

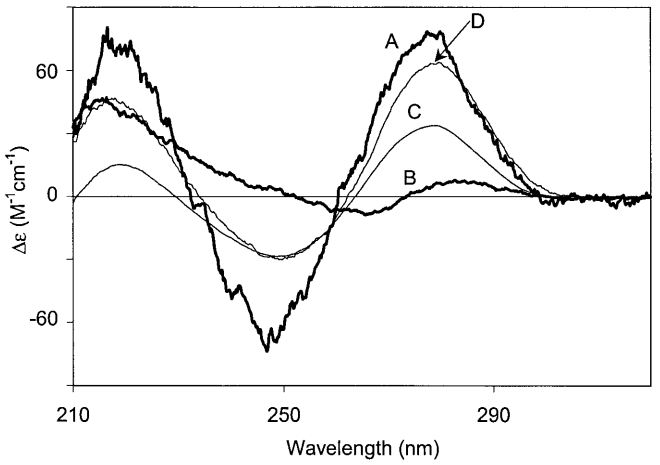

Fig. 8. UV CD spectra of different hairpins. A, AT[GA3] (▬); B, AT[GA3] with Cu(T4) at Hp/Cu = 1(▬); C, CG[GA3] (—); D, CG[GA3]with Cu(T4) at Hp/Cu = 1 (—).

3.3. Temperature studies

The temperature dependence of the absorption spectrum gives information about the hairpin-to-random coil transition. Fig. 9 shows the transition for free TT[T4] as observed at 260 nm. The loss of the stacking interactions among the bases accounts for the absorbance increase, and the assumption is that the process occurs with the unfolding of the hairpin. (Accordingly, a standard method for determining the

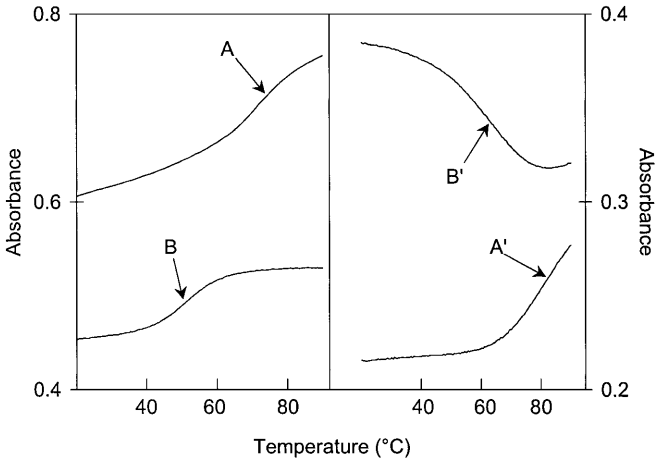

Fig. 9. Temperature dependent absorbance changes of selected hairpin samples with arrows marking the melting temperatures. A, CG[T4] monitored at 260 nm; A′, CG[T4] with Cu(T4) at Hp/Cu = 1 monitored at 424 nm; B, TT[T4] monitored at 260 nm; B′, TT[T4] with Cu(T4) at Hp/Cu = 1 monitored at 424 nm.

concentration assumes that at high temperature the numerical sum of the molar extinction coefficients of the participating bases gives a good approximation to the molar absorptivity of the oligonucleotide). Table 1 includes the melting temperature (T_m) that the curve implies for TT[T4] as well as data for other hairpins. Fig. 9 also shows that is possible to monitor the melting process in the presence of Cu(T4) in which case it is more convenient to follow the process at 424 nm. For adducts of the CG hairpins there is an increase in absorbance, while the absorbance decreases for other hairpins. As expected, the data in Table 1 indicate that the binding of Cu(T4) enhances the melting temperature. Fig. 10 shows the absorbance in the Soret region for Cu(T4) in the presence and the absensce of TT[T4] at 25 and 90°C. At 90°C the absorption maximum of the mixture of TT[T4] and Cu(T4) is similar to that observed for Cu(T4) combined with PU or PY.

4. Discussion

4.1. Hairpin structures

There are many applications for DNA hairpins as model substrates. Previous investigators have, for example, used hairpin structures to investigate the effect of conformation on DNA cleavage reactions with artificial nucleases [46–49]. Because of the stability a relatively short hairpin can exhibit, Jollès et al. have attached a hairpin-forming fragment at the 3′ end of an antisense oligonucleotide in attempts to stabilize the drug against intracellular nucleases [50]. Lewis and co-workers have exploited the framework by introducing a photoactive agent into the loop of a hairpin in order to study electron-transfer reactions with remote bases in the stem

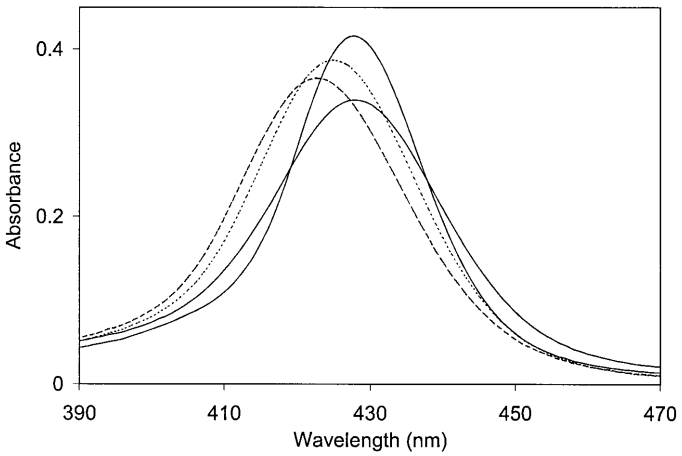

Fig. 10. Absorption spectra of Cu(T4). In order of decreasing intensity at the Soret maximum with TT[T4] at 20°C and Hp/Cu = 5 (—); without hairpin at 20°C (••); without hairpin at 90°C (– –); with TT[T4] at 90°C and Hp/Cu = 5 (—).

[51]. Doubly end-labeled hairpins are potentially useful as molecular sensors [52] and in the studies with Cu(T4), this laboratory has used hairpins in DNA-binding studies.

The stem of the 16-mers studied is a double helix with well defined minor and major grooves, but is only about two-thirds of a turn long. Two other important characteristics each structure should have are a compact loop, as shown by NMR studies [41,53], and uncharged ends. That is, there are no terminal phosphate groups on either the 3′ or the 5′ end of the chain. These constraints suggest that Cu(T4) is likely to bind towards the middle of the stem, where, in fact, the binding is quite sensitive to base substitution [43,54]. In any case, that is the justification for the base-replacement strategy employed.

Although such hairpin substrates offer many advantages for DNA-binding studies, there are some potential complications. The plusses include easy modification of specific atoms or functional groups within the duplex and the opportunity to vary the stability of the overall structure via modifications of the loop. In principle, structural determinations of adducts are also possible using NMR techniques. There are, however, a few questions to consider, (1) Is the loop a competitive domain that further complicates the system?; (2) Does the stem-loop structure even remain intact when Cu(T4) binds?; (3) Does the loop influence the binding interactions within the stem? More importantly, can a change in the loop fundamentally alter the nature of the adduct, viz. induce a switch from external to intercalative binding?

4.2. The loop aspect

The loop is, in essence, a single-stranded domain within the hairpin. Interaction with Cu(T4) is certainly feasible because Pasternack and co-workers have shown that the porphyrin binds to poly (A) [55]. However, the binding studies with PU and PY described herein, as well as the work with poly (A), show that interaction with single-stranded DNA leads to a modest bathochromic shift in the Soret band of Cu(T4) and a limited decrease in the absorbance ($H \approx 10\%$). With PU the emission from the Cu(T4) adduct is also quite weak as is the induced, negative CD signal. These findings suggest that the interaction with single-stranded DNA entails a limited amount of π stacking between the porphyrin and one or more bases of the oligonucleotide. Only partial internalization occurs, and the emission intensity is quite weak due to the easy access of the copper center. Since the interaction with a hairpin typically produces much greater changes in the absorbance, emission, and CD signals, the clear implication is that Cu(T4) binds in the stem region and that the DNA host retains double-stranded character. At higher temperatures, however, after the melting of the secondary structure, the absorbance data suggest that Cu(T4) binds to what is then essentially single-stranded material.

The next interesting question is does the loop determine the mode of binding in the stem. The short answer is not in a major way. Thus, for three very different loops the absorbance, emission and CD data all show that Cu(T4) consistently intercalates into CG hairpins and that the corresponding TT hairpins always

engage in external binding. The results for the AT hairpins require a little more discussion. Independent of the loop, the small bathochromic shifts and the hyperchromism in the Soret band as well as the uniformly weak emission intensities clearly point towards external binding. However, the CD signals of the adducts vary considerably. With AT[T4], uptake of Cu(T4) induces a positive signal in the Soret region as in the case of the TT hairpins. On the other hand, adduct formation with AT[GT2A] or AT[GA3] gives rise to a bisignate CD at all hairpin-to-porphyrin ratios. With random-sequence DNA [19] and other hairpins like TT[T4] or AT[T4], porphyrin–porphyrin interactions can give rise to a relatively strong, bisignate CD at low Hp/Cu values, but the signal becomes monosignate when there is excess of DNA to disperse the porphyrin. In the case of a conservative CD spectrum of that type, the crossover wavelength coincides with the wavelength of the absorption maximum [56]. For the adducts with AT[GT2A] or AT[GA3], however, the CD signal is relatively weak, and the crossover does not occur at the absorption maximum. Shreiner and co-workers have observed a bisignate CD from Pd(T4) and attributed it to a complex bound edge-on in the major groove at an ApT step [57]. Cu(T4) may form a similar adduct with the AT hairpins in question. The evidence is that the stem sequence dictates the mode of binding, i.e. whether the binding is internal (intercalation) or external (groove binding); however, the loop sequence can modulate the binding and affect the spectral properties.

4.3. Higher adducts

For the hairpin substrates, a ratio of Hp/Cu = 5 is sufficient to ensure 1:1 binding of Cu(T4). However, a hairpin is capable of binding more than one porphyrin. In the case of CG[T4], for example, the binding of a second Cu(T4) ion is evident from the overshoot in the hypochromism during the absorbance titration as well as from the gradual shift in the minimum that appears in the corresponding CD spectra. With the TT hairpins and with AT[T4], the formation of (at least) a 2:1 Cu(T4)/hairpin adduct at low Hp/Cu values accounts for the excitonic coupling interaction and the bisignate CD. However, the hyperchromism in the absorbance spectrum of the AT[T4] adduct under the same conditions is typical of an ordinary, externally bound Cu(T4) ion. In view of the fact that the porphyrin–porphyrin interactions appear to be of a relatively long range nature, the term 'outside stacking' [19,58] is probably not a very apt description of the multimer, at least with the hairpin substrates.

4.4. Externally bound Cu(T4)

Hairpins that are rich in A=T base pairs tend to support external, or groove binding, of Cu(T4) according to all the spectroscopic indicators. Table 2 contains representative data for AT-rich hairpins. The results reveal that a run of four A=T base pairs is clearly adequate for external binding, but not necessary. With a manganese analogue of Cu(T4), Muenier and co-workers interpret cutting data to establish that a triplet run is sufficient to define a relatively high affinity, external

binding site [59]. A hyperchromic response as a result of adduct formation is a clear sign that no significant stacking interaction occurs. Hyperchromism in the Soret region may not always occur with external binding to DNA but is a sure sign of that mode of interaction.

In contrast to the regular behavior of the Soret absorbance band, the induced CD signal of externally bound Cu(T4) can apparently be bisignate or possibly even weakly negative, vide infra. The understanding of the CD results is far from complete. For those adducts with a positive induced CD signal, the CD maximum generally does not coincide with the absorption maximum and occurs at a shorter wavelength (Table 2). In the case of the adduct with AT[GA3] or AT[GT2A] both extrema of the CD response fall below the absorption maximum. That may not be consistent with a single type of binding. The UV CD spectrum may be a useful indicator if aggregation of the porphyrin is not a problem at Hp/Cu = 1. The results reported above indicate that, compared with the free hairpin, external binding of Cu(T4) produces a definite decrease of $\Delta\varepsilon$ in the region of 280 nm. This effect could relate to the induced CD response in the visible region of Cu(T4), but conformational changes in the DNA are a potential complication [60].

4.5. Intercalation of Cu(T4)

Hairpins with stems that contain at least 50% G≡C base support intercalative binding of Cu(T4). The spectroscopic signatures of intercalation include a bathochromic shift of ≥ 8 nm in the Soret region and a hypochromic response of $H \geq 20$, as well as a negative induced CD signal with $\Delta\varepsilon \leq 20\ M^{-1}\ cm^{-1}$ (Table 2). In contrast to the response of the externally bound form, intercalated Cu(T4) has absorption and CD maxima at the same wavelength. Intercalative binding also gives rise to a pronounced increase of $\Delta\varepsilon$ in the CD spectrum at around 280 nm. Carvlin and Fiel have reported that a similar effect occurs at low loading of H_2T4 on $[poly(dG\text{-}dC)]_2$ [58]. A stem with a GpC or a CpG step supports intercalation as well as the AG and CA hairpins which do not contain contiguous G≡C base pairs. The common trend is that stems with a robust hydrogen-bonding framework support intercalation [43]. However, the rigidity criterion relates to the stem. High melting hairpins with stable loops like TT[GA3] do not support intercalation.

The other spectroscopic indication of intercalative binding is the observation of significant emission intensity from bound Cu(T4). The emission signal is weak in absolute terms, with a quantum yield of no more than about 10^{-4}, but contrasts sharply with that of the free copper porphyrin which is virtually non-emissive in aqueous solution [24]. Lewis bases quench the emission by transiently coordinating at an axial position of the copper complex. In the five-coordinate form a d–d excited state drops below the emissive π–π^* state, and the upshot is dramatically enhanced non-radiative decay [24]. Quenching is almost as efficient for the externally bound porphyrin either because of axial coordination of solvent or a basic atom on the surface of the DNA [61]. However, intercalative binding preserves the four-coordinate structure and permits observation of the emission. It is possible that fluctuations of the structure permit intermittent access to axial coordination

sites of the copper center. That could explain why the emission intensity is greater when Cu(T4) intercalates into hairpins like CG[GT2A] and CG[GA3], which have higher melting temperatures. Also, of the hairpins with a [T4] loop that support intercalation, the emission intensity tends to be higher for systems like CG or GC than for AG or CA. Note that the latter have fewer G≡C base pairs and melt at lower temperatures.

4.6. Role of hydrogen bonding

With hairpin substrates it is possible to probe the role of the internal hydrogen-bonding framework by judicious replacement of guanine with inosine. Scheme 2 shows guanine, which relies upon hydrogens of the amino group and N1 along with a lone pair of the carbonyl oxygen to form three hydrogen bonds to cytosine. Inosine, the same purine except without the amino substituent also binds selectively to cytosine but forms only two hydrogen bonds. The labels CI and AI stand for the modified hairpins that incorporate inosine in designated locations:

$$\mathrm{CI} = \frac{\mathrm{GACIAC^TT}}{\mathrm{CTICTG_TT}} \qquad \mathrm{AI} = \frac{\mathrm{GAAIAC^TT}}{\mathrm{CTTCTG_TT}}$$

By comparison with the CG and AG analogues base replacement lowers the melting temperature by about 12°C due to the reduction in the number of hydrogen bonds in the stem, More importantly, there are marked differences in the binding of Cu(T4) [54]. The most dramatic effect occurs with CI. Whereas Cu(T4) intercalates into the CG hairpin the results in Table 2 unambiguously show that the porphyrin binds externally to the CI analogue. In line with external binding the Soret band also shows a small bathochromic shift and hyperchromism when Cu(T4) binds to the AI hairpin. With both the CI and AI adducts there is almost complete quenching of the emission as well. However, the induced CD signal is a weak negative band for the adduct with AI. The simplest interpretation is that a fraction of the total porphyrin intercalates into the hairpin and dominates the CD

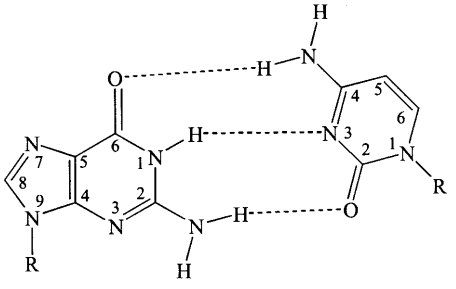

Guanine Cytosine

Scheme 2.

response. In keeping with the explanation, the emission excitation spectrum maximizes at 433 nm. On the other hand, the absorption maximum occurs at 429 nm, so the bulk of the porphyrin must bind externally.

The IC hairpin is different in that the maxima in the absorption, CD and excitation spectra all agree fairly closely, so there appears to be only one type of adduct present. It is tempting to conclude that the IC host engages in some sort of stacking interaction with the Cu(T4) guest because of the modest degree of hypochromism (Table 2). Consistent with this possibility the emission signal is noticeably stronger than those obtained with the other inosine-containing systems, though quite a bit weaker than that of the analogous GC adduct.

The results with the IC hairpin not withstanding the inosine-for-guanine replacement experiments clearly establish the critical role that a robust hydrogen-bonding framework plays in supporting the intercalative binding of Cu(T4). The most remarkable comparison involves the AG and the AI hairpins where the deletion of just one out of a total of at least 15 hydrogen bonds in the stem leads to a complete redirection of the binding of Cu(T4).

4.7. Structure considerations

Externally binding organic ions generally interact within one of the grooves that wind around the surface of the DNA host. The attractive forces may include the electrostatic potential due to the sugar–phosphate backbone the hydrophobic effect, hydrogen-bonding to atoms along the floor of the groove and/or van der Waals interactions. One of the earliest proposals for the binding of molecules like Cu(T4) was a face-on interaction within the major groove [15]. Subsequently obtained time-resolved Raman results are consistent with this model [61]. On the other hand the results with derivatives of Mn(T4) that act as artificial nucleases are consistent with edge-on binding in the minor groove [59,62,63]. Typically, metalloporphyrins do not have the crescent shape of a classical groove binder, so groove binding is apt to be most efficacious when the local DNA structure can conform to the shape of the porphyrin so as to give an 'induced fit'. Consistent with this reasoning, the sequences that most readily support external binding of Cu(T4) are rich in A=T base pairs which are relatively flexible because they have only two hydrogen bonds between bases. In the words of Pasternack and co-workers a flexible polymer like [poly (dA-dT)]$_2$ is 'able to bend, flex, or kink around molecules bound externally in its minor groove' [29]. Such deformations amount to a partial melting of the local DNA structure. However, flexibility of the double helix is sequence dependent; for example, an ApT step tends to be more rigid than a TpT or a TpA step [64]. In addition the choice of loop can influence the flexibility in the case of a hairpin substrate. Steric constraints also vary with the base composition [65], as well as the porphyrin. It would, therefore, hardly be surprising if the shape and location of the ideal binding pocket were to differ for a metalloporphyrin without axial ligands as opposed to a derivative with one or even two axial ligands, Consistent with this hypothesis the binding studies with Cu(T4) and the TT, AT[GT2A] and IC hairpins as well as work with a palladium analogue [57] suggest

that the shape of the induced CD signal varies for different externally bound adducts.

The energy factors involved in intercalative binding include the cost of cavity creation, the hydrophobic effect associated with the transfer of the aromatic reagent from the bulk medium, as well as specific interaction [66]. Most evident among the latter are the coulombic terms, the van der Waals energy, and, quite importantly for porphyrins like Cu(T4), steric effects. In an early work Fiel and Munson proposed that the intercalation of a molecule like H_2T4 involves wedging the core of the porphyrin between base pairs in a symmetrical fashion so that two of the peripheral pyridyl substituents lie in the minor groove and two in the major groove [15]. Later calculations by Hui et al. supported this model [67]. Some direct structural information finally became available in 1996 when Williams and co-workers solved the crystal structure of a 2:1 adduct of Cu(T4) with $[d(CGATCG)]_2$ [31]. The structure confirmed some of the original expectations but there were surprises. Most striking was the number of van der Waals contacts that occur among atoms of the pyridyl groups and the sugar–phosphate backbone in the minor groove. The steric congestion causes the duplex to unravel at both ends and to extrude the 5′-terminal cytidines. Lipscomb et al. proposed that such base extrusion would inevitably occur, even in solution, and they invoked the term 'hemi-intercalation' to describe the binding motif [31]. The solution results are, however, not directly comparable to solid-state models where hydrogen-bonding between neighboring duplexes is possible.

Irrespective of the mode of interaction, DNA must adapt its conformation in order to take up Cu(T4), and only sequences that contain at least 50% G≡C base pairs support intercalation. An advantage of intercalative binding is that the DNA can essentially retain a B-form structure, but steric problems arise with molecules like Cu(T4). As a consequence, the intercalation of the porphyrin is only feasible if there is a robust hydrogen-bonding framework present to dictate the structure. It follows that hemi-intercalation is unlikely to occur in solution because the extrusion of cytidine involves breaking the hydrogen bonds that are necessary to promote internalization in the first place. On the other hand, the existence of adjacent G≡C base pairs is not a requirement for an intercalation site. The presence of such a step does enhance the rigidity, though, and consequently promotes greater emission intensity from intercalated Cu(T4). As a rule, the emission intensity increases with the rigidity, and for hairpins, even the loop structure has an impact. Thus, the adducts of the CG[GT2A] and CG[GA3] hairpins exhibit the highest emission yields, about twice that of the adduct with CG[T4]. Indications are that deintercalation is a relatively slow process with such porphyrins [68], but the more fluid the structure, the more likely is the exposure of the axial coordination positions of the copper center. If it turns out that Cu(T4) intercalates into IC[T4], the range of observable emission intensities is large indeed. The proximity of at least one G≡C base pair is apparently necessary in order for the local structure to be rigid enough to observe emission intensity from the intercalated Cu(T4) ion.

A simple bifurcation of Cu(T4) adducts into intercalated or groove-bound categories is probably an oversimplification. These two motifs may only be the

extremes of an array of structures wherein the degree of internalization varies almost continuously. For example, partial melting of the canonical DNA structure may expose one or more bases and facilitate some types of stacking interaction even when the porphyrin remains essentially surface bound. The caveat in that the observation of hypochromism and a negative induced CD band in the Soret region may only be necessary, as opposed to sufficient, conditions for characterizing an intercalative binding interaction. Indeed, Lincoln and Nordén have proposed several non-traditional types of interactions that could lead to stacking interactions involving DNA bases [69]. The classification of any particular adduct will generally require studies utilizing multiple physical methods.

5. Conclusions

Hairpin substrates have proven to be useful vehicles for studying DNA-binding interactions with Cu(T4). The significant findings include, (1) Hairpin stems define short, but stable of runs of B-form DNA, that retain double-stranded character in the adducts; (2) Cu(T4) will intercalate into a duplex that contains at least 50% G≡C base pair regardless of the sequence; (3) If, on the other hand, the duplex contains more than 50% A=T base pairs, the porphyrin tends to bind externally; (4) The most important factor that shapes the binding is the local rigidity of the DNA. The flexibility of A=T base pair facilitates DNA distortions and formation of an external binding pocket for the porphyrin. In contrast, the enhanced hydrogen bonding in G≡C rich sequences reinforces the B-form structure and biases the DNA towards intercalative binding of Cu(T4) in spite of steric clashes that occur in the minor groove; (5) Alterations in the composition of the loop affect the rigidity of the structure and the spectral properties of the adduct, but the fundamental binding motif of Cu(T4) generally does not change.

Acknowledgements

The National Science Foundation supported this research through grant number CHE-9726435. PLP was the recipient of a Sloan Foundation fellowship administered by Purdue University. Joseph F. Michalec helped a great deal in formatting the figures. The detailed comments of a reviewer were very helpful in clarifying the presentation.

References

[1] R.J. Fiel, J. Biomol. Struct. Dyn. 6 (1989) 1259.
[2] L.G. Marzilli, New J. Chem. 14 (1990) 409.
[3] R.F. Pasternack, E.J. Gibbs, Met. Ions Biol. Syst. 33 (1996) 367.
[4] D.R. McMillin, K.M. McNett, Chem. Rev. 98 (1998) 1201.

[5] I. Haq, J.O. Trent, B.Z. Chowdhry, T.C. Jenkins, J. Am. Chem. Soc. 121 (1999) 1768.
[6] F.X. Han, R.T. Wheelhouse, L.H. Hurley, J. Am. Chem. Soc. 121 (1999) 3561.
[7] C. Kasturi, M.S. Platz, Photochem. Photobiol. 56 (1992) 427.
[8] G. Pratviel, M. Pitié, J. Bernadou, B. Meunier, Angew. Chem. Int. Ed. Engl. 30 (1991) 702.
[9] B.R. Munson, R.J. Fiel, Nucleic Acids Res. 20 (1992) 1315.
[10] J. Miller, J. Chem. Edu. 76 (1999) 592.
[11] B.W. Henderson, T.J. Dougherty, Photochem. Photobiol. 55 (1992) 147.
[12] D.T. Croke, L.A. Perrouault, M.A. Sari, J.P. Battioni, D. Mansuy, C. Hélène, T. Ledoar, J. Photochem. Photobiol. B Biol. 18 (1993) 41.
[13] J.B. Verlhac, A. Gaudemer, I. Kralji, Nouv. J. Chim. 8 (1984) 401.
[14] R.J. Fiel, J.C. Howard, E.H. Mark, N. Datta-Gupta, Nucleic Acids Res. 6 (1979) 3093.
[15] R.J. Fiel, B.R. Munson, Nucleic Acids Res. 8 (1980) 2835.
[16] D.L. Banville, L.G. Marzilli, W.D. Wilson, Biochem. Biophys. Res. Commun. 113 (1983) 148.
[17] M.J. Carvlin, R.J. Fiel, Nucleic Acids Res. 11 (1983) 6121.
[18] R.F. Pasternack, E.J. Gibbs, J.J. Villafranca, Biochemistry 22 (1983) 2406.
[19] M.J. Carvlin, N. Datta-Gupta, R.J. Fiel, Biochem. Biophys. Res. Commun. 108 (1982) 66.
[20] N.E. Geacintov, V. Ibanez, M. Rougee, R.V. Benasson, Biochemistry 26 (1987) 3087.
[21] L.G. Marzilli, D.L. Banville, G. Zon, W.D. Wilson, J. Am. Chem. Soc. 108 (1986) 4188.
[22] G.D. Strahan, D. Lu, M. Tsuboi, K. Nakamoto, J. Phys. Chem. 96 (1992) 6450.
[23] J.M. Kelly, M.J. Murphy, D.J. McConnel, C. OhUigin, Nucleic Acids Res. 13 (1985) 167.
[24] B.P. Hudson, J. Sou, D.J.M. Berger, D.R. McMillin, J. Am. Chem. Soc. 114 (1992) 8997.
[25] J.A. Strickland, L.G. Marzilli, W.D. Wilson, Biopolymers 29 (1990) 1307.
[26] B. Ward, A. Skorobogaty, J.C. Dabrowiak, Biochemistry 25 (1986) 7827.
[27] K. Ford, K.R. Fox, S. Neidle, M.J. Waring, Nucleic Acids Res. 15 (1987) 2221.
[28] J.A. Strickland, D.L. Banville, W.D. Wilson, L.G. Marzilli, Inorg. Chem. 26 (1987) 3398.
[29] E.J. Gibbs, M.C. Maurer, J.H. Zhang, W.M. Reiff, D.T. Hill, M. Malcika-Blaszkiewicz, R.E. McKinnie, H.Q. Liu, R.F. Pasternack, J. Inorg. Biochem. 32 (1988) 39.
[30] N.N. Kruk, S.I. Shishporenok, A.A. Korotky, V.A. Galievsky, V.S. Chirnovy, P.Y. Turpin, J. Photochem. Photobiol. B Biol. 45 (1998) 67.
[31] L.A. Lipscomb, F.X. Zhou, S.R. Presnell, R.J. Woo, M.E. Peek, R.R. Plaskon, L.D. Williams, Biochemistry 35 (1996) 2818.
[32] M.A. Fountain, M.J. Serra, T.R. Krugh, D.H. Turner, Biochemistry 35 (1996) 6539.
[33] L.E. Xodo, G. Manzini, F. Quadrifogiio, G.A. van der Marel, J.H. van Boom, Biochemistry 27 (1988) 6321.
[34] D. Rentzeperis, K. Alessi, L.A. Marky, Nucleic Acids Res. 21 (1993) 2683.
[35] J. Petruska, N. Arnheim, M.F. Goodman, Nucleic Acids Res. 24 (1996) 1992.
[36] T.M. Davis, L. McFail-Isom, E. Keane, L.D. Williams, Biochemistry 37 (1998) 6975.
[37] S. Takenaka, M. Yokoyama, H. Kondo, Chem. Commun. (1997) 115.
[38] C.W. Hilbers, H.A. Heus, M.J.P. van Dongen, S.S. Wijmenga, Nucleic Acids Mol. Biol. 8 (1994) 56.
[39] M.M. Senior, R.A. Jones, K.J. Breslauer, Proc. Natl. Acad. Sci. USA 85 (1988) 6242.
[40] V.P. Antao, S.Y. Lai, I. Tinoco Jr, Nucleic Acids Res. 19 (1991) 5901.
[41] M.J.P. van Dongen, M.M.W. Moorem, E.F.A. Willems, G.A. van der Marel, J.H. van Boon, S.S. Wijmenga, C.W. Hilbers, Nucleic Acids Res. 25 (1997) 1537.
[42] M.J.J. Blommers, J.A.L.I. Walters, C.A.G. Haasnoot, J.M.A. Aelen, G.A. van der Marel, J.H. van Boom, C.W. Hilbers, Biochemistry 28 (1989) 7491.
[43] M.K. Eggleston, D.K. Crites, D.R. McMillin, J. Phys. Chem. A 102 (1998) 5506.
[44] J. Sambrook, E.F. Fritsch, T. Maniatis, Molecular Cloning: A Laboratory Manual, Cold Spring Laboratory Press, Cold Spring Harbor, NY, 1989, pp. E.1–E.2.
[45] J.G. Nadeau, P.T. Gilham, Nucleic Acids Res. 13 (1985) 8259.
[46] C.J. Burrows, S.E. Rokita, Acc. Chem. Res. 27 (1994) 295.
[47] S.A. Ciftan, H.H. Thorp, J. Am. Chem. Soc. 120 (1998) 9995.
[48] P.J. Carter, C.-C. Cheng, H.H. Thorp, Inorg. Chem. 35 (1996) 3348.
[49] J.G. Muller, P. Zheng, S.E. Rokita, C.J. Burrows, J. Am. Chem. Soc. 118 (1996) 2320.

[50] B. Jollès, M. Réfrégiers, A. Laigle, Nucleic Acids Res. 25 (1997) 4608.
[51] F.D. Lewis, S.A. Helvoight, R.L. Letsinger, Chem. Commun. (1999) 327.
[52] G. Bonnet, S. Tyagi, A. Libchaber, F.R. Kramer, Proc. Natl. Acad. Sci. USA 96 (1999) 6171.
[53] C.A.G. Haasnoot, S.H. de Bruin, R.G. Berendsen, H.G.J.M. Janssen, T.J.J. Binnendijk, C.W. Hilbers, J. Biomol. Struct. Dyn. 1 (1983) 115.
[54] D.K. Crites-Tears, D.R. McMillin, Chem. Commun. (1998) 2517.
[55] R.F. Pasternack, R.A. Brigandi, M.J. Abrams, A.P. Williams, E.J. Gibbs, Inorg. Chem. 29 (1990) 4483.
[56] C.R. Cantor, P.R. Schimmel, Biophysical Chemistry, Freeman, San Francisco, 1980, pp. 418–425.
[57] N.R. Barnes, P.D. Stroud, K.E. Robinson, C. Horton, A.F. Schreiner, Biospectroscopy 5 (1999) 179.
[58] M.J. Carvlin, E. Mark, R.J. Fiel, Nucleic Acids Res. 11 (1983) 6141.
[59] G. Pratviel, J. Bernadou, B. Meunier, Angew. Chem. Int. Ed. Engl. 34 (1995) 746.
[60] M. Lin, M. Lee, K.T. Yue, L.G. Marzilli, Inorg. Chem. 32 (1993) 3217.
[61] P. Mojzes, L. Chinsky, P.Y. Turpin, J. Phys. Chem. 97 (1993) 4841.
[62] U. Sehlstedt, S.K. Kim, P. Carter, J. Goodisman, J.F. Vollano, B. Nordén, J.C. Dabrowiak, Biochemistry 33 (1994) 417.
[63] G. Pratviel, J. Bernadou, B. Meunier, Adv. Inorg. Chem. 45 (1998) 251.
[64] M. Suzuki, N. Yagi, J.T. Finch, FEBS Lett. 379 (1996) 148.
[65] K.G. Ford, L.H. Pearl, S. Neidle, Nucleic Acids Res. 15 (1987) 6553.
[66] J.B. Chaires, Biopolymers 44 (1997) 201.
[67] X. Hui, N. Gresh, B. Pullman, Nucleic Acids Res. 18 (1990) 1109.
[68] R.F. Pasternack, E.J. Gibbs, J.J. Villafranca, Biochemistry 22 (1983) 5409.
[69] P. Lincoln, B. Nordén, J. Phys. Chem. B. 102 (1998) 9583.
[70] D.K. Crites, Ph.D. Thesis, Purdue University, 1998.